INGEMMET
INSTITUTO GEOLÓGICO, MINERO Y METALÚRGICO

OBSERVATORIO
VULCANOLÓGICO
INGEMMET

VIII FORO INTERNACIONAL
LOS **VOLCANES**
Y SU **IMPACTO**

Arequipa, 26 y 27 de abril del 2018

# LIBRO DE RESÚMENES

**Editor:**
**Rigoberto Aguilar**

AMPERE®

# dMODELS: a free software package to model volcanic deformation

**Maurizio Battaglia**[1,2]

[1] *Volcano Disaster Assistance Program, U.S. Geological Survey, Menlo Park, Calif., USA – mbattaglia@usgs.gov*
[2] *Dipartimento di Scienze della Terra, Sapienza – Università di Roma, Roma, Italia*

**Key words:** deformation, mathematical models, volcanoes.

## INTRODUCTION

Shallow magma accumulation in the crust often results in slight movements of the ground surface that can be measured using standard land-surveying techniques or satellite geodesy. Volcano geodesy uses measurements of crustal deformation to investigate volcano unrest and to search for magma reservoirs beneath active volcanic areas. A key assumption behind geodetic monitoring is that ground deformation of the Earth's surface reflects tectonic and volcanic processes at depth (e.g., fault slip and/or mass transport) transmitted to the surface through the mechanical properties of the crust.

Measurements and modeling of ground deformation are an indispensable component for any volcano monitoring strategy. The critical questions that emerge when monitoring volcanoes are how to (a) constrain the source of unrest, (b) improve the assessment of hazards associated with the unrest and (c) refine our ability to forecast volcanic activity.

A number of analytical and numerical mathematical models are available in the literature that can be used to fit ground deformation to infer source location, geometry, depth and volume change. Analytical models offer a closed-form description of the volcanic source. This allows us, in principle, to readily infer the relative importance of any of the source parameters. The careful use of analytical models, together with high quality data sets can provide valuable insights into the nature of the deformation source (e.g., Battaglia and Hill, 2009).

The simplifications that make analytical models tractable, however, may result in misleading interpretations. Sources are approximated by pressurized cavities in homogenous, elastic half-spaces filled with fluids. Although actual magmatic sources are certainly more complex, this approach can mimic the stress or potential field of the magma or other fluid sources beneath a volcano.

The use of numerical models (e.g., finite element models) allows for evaluation of more realistic source characteristics and crustal properties (e.g., vertical and lateral mechanical discontinuities, complex source geometries, topography) but may require expensive proprietary software and powerful computers.

## dMODELS

The dMODELS software package provides MATLAB functions and scripts to (1) compute internal and surface deformation, internal and surface strain, and surface tilt due to a pressurized source or rectangular dislocation in a homogenous, isotropic, elastic, flat half-space; (2) invert GPS, InSAR and tilt data for spherical, spheroidal and sill-like pressure sources and (3) utilities to transform between coordinate systems, create vector plots of GPS deformation velocities and create kml files that can be imported in Google Earth (Figure 1; Battaglia et al., 2013).
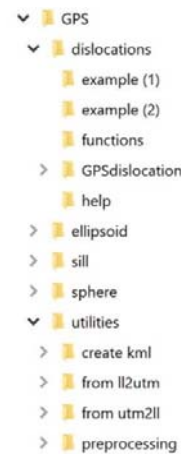


Fig. 1 – Example of directory tree for the GPS module of dMODELS. See text for a description of the source geometries and utilities implemented in the module.

Surface deformation due to an expanding or contracting magma chamber has frequently been modeled by a dilatation point source in an elastic half space (the so-called Mogi's source). The dMODELS software package implements the more general model for a finite (pressurized) spherical source. The model simulates a small spherical source embedded in a homogeneous, isotropic, elastic space with a first order correction for topography. The analytical solution implemented in dMODELS includes higher-order terms taking into account the finite shape of a spherical body; thus,

the local stresses at, and away from, the boundary of a chamber can be calculated (unlike the point source case). The spherical source is described by four parameters: volume change, location (2 parameters) and depth.

A simple model of an active volcanic system might include two principal elements: a magma reservoir and a conduit through which magma may reach the surface, approximated by a prolate spheroid. The solution for a prolate spheroid depends on seven parameters: the dimensionless pressure change, the geometric aspect ratio between the semi-major axis a and the semi-minor axis b, the source location (2 parameters), the dip angle (measured from the free surface) and the azimuth angle (measured clockwise from the positive North direction).

A simple 3-D model of a horizontal sill-like intrusion is a horizontal penny-shaped crack in a semi-infinite elastic body. The dMODELS software package implements approximate expressions for a horizontal sill. These are appropriate for a horizontal sill-like source whose radius is up to five times larger than its depth. The solution for a horizontal penny-shaped crack depends on five parameters: the dimensionless pressure change, the crack radius, the source location (2 parameters) and depth.

Finally, dMODELS implements the complete suite of closed analytical expressions for the internal and surface displacements and tilts due to a strike-slip, dip-slip or tensile rectangular dislocation. These expressions are particularly compact and free from singular points. They can be used to model deformation related to fault slip as well as the intrusion of rectangular dikes. The solution for a dislocation depends on eight parameters: displacement, initial and end points (4 parameters), dip angles, top and bottom depths.

## CASE STUDY

Augustine Volcano, in the lower Cook Inlet (275 km southwest of Anchorage, Alaska), is a 1200-m-high dacitic stratovolcano consisting of a central dome complex, lava flows, and pyroclastic deposits. On January 11, 2006, the volcano erupted after nearly 20 years of quiescence. No deformation had been observed at Augustine since the 1986 eruption until renewed unrest began in early summer 2005. Continuous GPS instrumentation at Augustine (Figure 2) measured clear precursory deformation consistent with a source of inflation or pressurization beneath the volcano's summit at a depth around sea level (Cervelli et al., 2006).



Fig. 2 – Map of the permanent GPS monitoring network of Augustine volcano (Alaska) created using the dMODELS utility "create kml."

Deformation at Augustine volcano can be divided in three intervals: (1) precursory deformation between Julian day 184 2005 and 320 2005; (2) volcanic unrest (constant deformation velocity) from Julian 321 2005 to 010 2006; (3) a sudden increase of the deformation velocity from Julian 011 2006 (beginning of the eruption); see Figure 3.
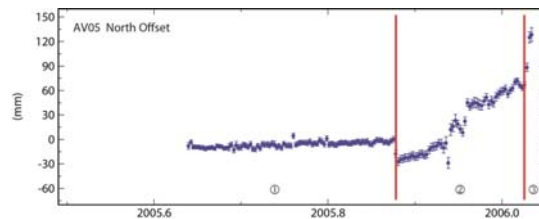


Fig. 3 – Permanent GPS time series showing the three different stages of unrest at Augustine volcano (Alaska).

Visual inspection of the deformation field during the early precursory stage showed a radial pattern in the horizontal deformation (Figure 4).
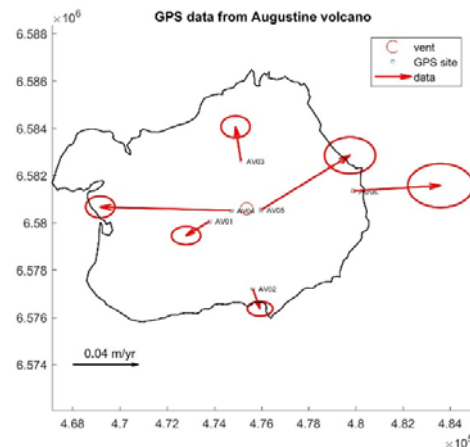


Fig. 4 – Vector plot of the GPS deformation velocities created using the utility "preprocessing."

To determine the parameters of the intrusion, we jointly invert the GPS horizontal and vertical deformation velocities measured between June 2005 and January 28, 2006 (Figure 4) using a non-linear weighted least-square algorithm with a random search grid. We invert using each model separately, and then compare the results (Table 1). Measurement errors are coded in the covariance matrix and the penalty function is the chi-square per degrees of freedom. The minimum of the penalty function is determined using the interior-point algorithm (Figure 5).
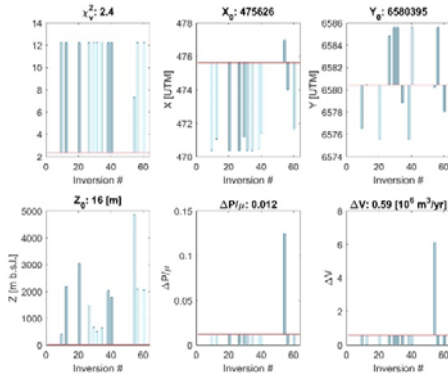


Fig. 5 – Stair-step plot of the inversion results for a spherical source (top: chi square per degrees of freedom, source location; bottom: source depth, dimensionless pressure change and volume change). The plot shows the distribution of the results for the random search grid algorithm. The title of each subplot gives the best fit value of the parameters. Created by the dMODEL script GPSSphereTopo.m.
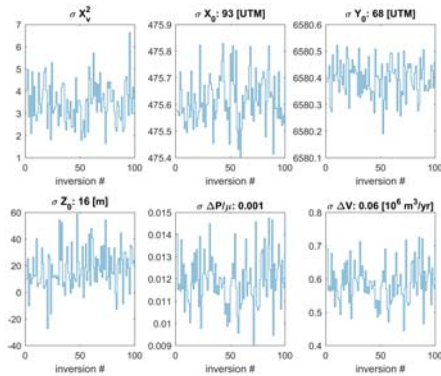


Fig. 6 – Stair-step plot of the results for the error estimate for the parameters of a spherical source. See also Figure 5. Created by the dMODEL script GPSSphereTopo.m.

Errors for the source parameters are determined using a Monte Carlo simulation technique. We determine 100 best-fit solutions by inverting the original data set plus noise. The noise for each data point was created using a normal distribution with zero mean and standard deviation equal to the data uncertainty. Uncertainties listed in Figure 6 are the standard deviation of the distribution of the 100 best-fit solutions found.

We test four source geometries (Table 1): a spherical source, a prolate spheroid, a horizontal penny-shaped source and an opening dike, all in an elastic, homogeneous, isotropic half-space.

Table 1. Source parameters

|  | Dike | Sill | Sphere | Spheroid |
|---|---|---|---|---|
| $\chi_v^2$ | 2.0 | 2.0 | 2.4 | 3.5 |
| Np [1] | 8 | 5 | 4 | 7 |
| X [2] [m] |  | 96 | 259 | -87 |
| Y [2] [m] |  | -184 | -196 | -170 |
| Depth [3] [m] |  | 1100 | 1188 | 1100 |
| ΔV [×$10^6$ m³] |  | 0.60 | 0.59 | 0.66 |
| Radius [m] |  | 105 |  |  |
| A |  |  |  | 1 |
| Strike [°] |  |  |  | 22 |
| Dip [°] | 2 |  |  | 90 |
| Xi [1] [m] | -1433 |  |  |  |
| Yi [1] [m] | -2722 |  |  |  |
| Xe [1] [m] | 4707 |  |  |  |
| Ye [1] [m] | 2965 |  |  |  |
| Displacement [m] | 1 |  |  |  |
| Top [2] [m] | 1100 |  |  |  |
| Bottom [2] [m] | 1110 |  |  |  |

[1] Number of independent parameters
[2] Relative to the vent
[3] Below the vent

We compare the proposed models by performing F-tests (e.g., Battaglia and Hill, 2009) on the residual. To test if the reduction in the error $\chi_v^2$ is greater than would be expected simply because additional model parameters were added, the F-variable

$$F_{(Np_x - Np_{Sphere}),v_x} = \frac{\left(\chi_{v\,Sphere}^2 v_{Sphere} - \chi_{v\,X}^2 v_X\right)\big/\left(Np_X - Np_{Sphere}\right)}{\chi_{v\,X}^2}$$

is used, where $X$ indicates the dike or sill-like source, $v$ are the degrees of freedom, and $Np$ the number of source parameters (4 for a sphere, 5 for a sill and 8 for a dike). The F-variable is expected to

follow the statistical distribution of a F-function with $Np_X - Np_{sphere}$ versus $v_X$ degrees of freedom. The experimental value of F is compared to a reference value with less than a 1% probability of being exceeded by chance. In Figure 7, we use the spherical model (which has the fewest parameters) as our null hypothesis (a sphere is the source geometry best-fitting the data). If the experimental value exceeds the reference value, then there is a 99% probability that the null-hypothesis is violated (a sphere is not source geometry best-fitting the data; a more complex source geometry is needed to explain the surface deformation).
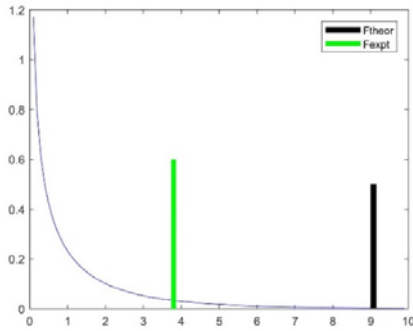


Fig. 7 – Example of F-test run by the "F-test" utility of dMODELS. The test compares the fit of a sill-like source (5 parameters) against that of a spherical source (4 parameters).



Figure 8. Vector plot showing the fit between the experimental (red vectors) and modeled (blue vectors) horizontal deformation velocities. Error ellipses correspond to 1 standard deviation. The best fit source is a spherical source at a depth of 16 m above sea level and a volume change of $0.59 \times 10^6$ m$^3$.

Figure 7 shows that the experimental value of F is smaller than the theoretical value. This means that the null-hypothesis is verified: a pressurized spherical source (described by 4 parameters only)

can satisfactorily fit and explain the surface deformation; even if has a smaller error, the more complex sill-like source (described by 5 parameters) is not adding any significant information about the source of the deformation (Table 1, Figure 8 and Figure 9).
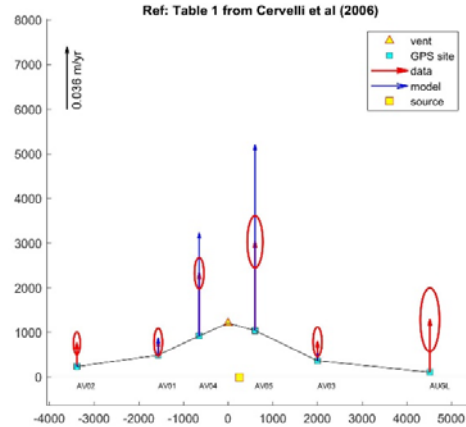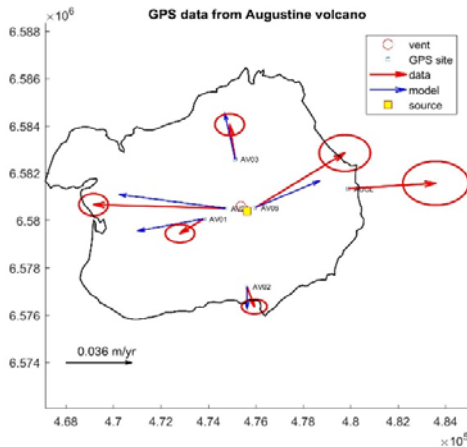


Figure 9. Vector plot showing the fit between the experimental (red vectors) and modeled (blue vectors) vertical deformation velocities. Error ellipses correspond to 1 standard deviation. The best fit source is a spherical source at a depth of 16 m above sea level and a volume change of $0.59 \times 10^6$ m$^3$.

## Acknowledgments

## References

Battaglia, M., Hill, D. P., (2009). Analytical modeling of gravity changes and crustal deformation at volcanoes: The Long Valley caldera, California, case study. Tectonophysics 471, 45-57.

Battaglia, M., Cervelli, P. F., Murray, J. R. (2013). dMODELS: A MATLAB software package for modeling crustal deformation near active faults and volcanic centers. Journal of Volcanology and Geothermal Research, 254, 1-4.

Cervelli, P. F., Fournier, T., Freymueller, J., Power, J. A. (2006). Ground deformation associated with the precursory unrest and early phases of the January 2006 eruption of Augustine Volcano, Alaska. Geophysical Research Letters, 33(18).